Electronic Supplementary Material (ESI) for Physical Chemistry Chemical Physics.


**Supporting Information** for

# Synthesis, Properties, and Formation Mechanism of Mn-doped $Zn_2SiO_4$ nanowires and Associated Heterostructures

Haiqing Liu,[a] Dominic Moronta,[a] Luyao Li,[a] Shiyu Yue,[a] and Stanislaus S. Wong[a,*]

[a]Department of Chemistry, State University of New York at Stony Brook,
Stony Brook, NY 11794-3400, USA

*To whom correspondence should be addressed. Phone: 631-632-1703; 631-344-3178
Email: Stanislaus.wong@stonybrook.edu; sswong@bnl.gov

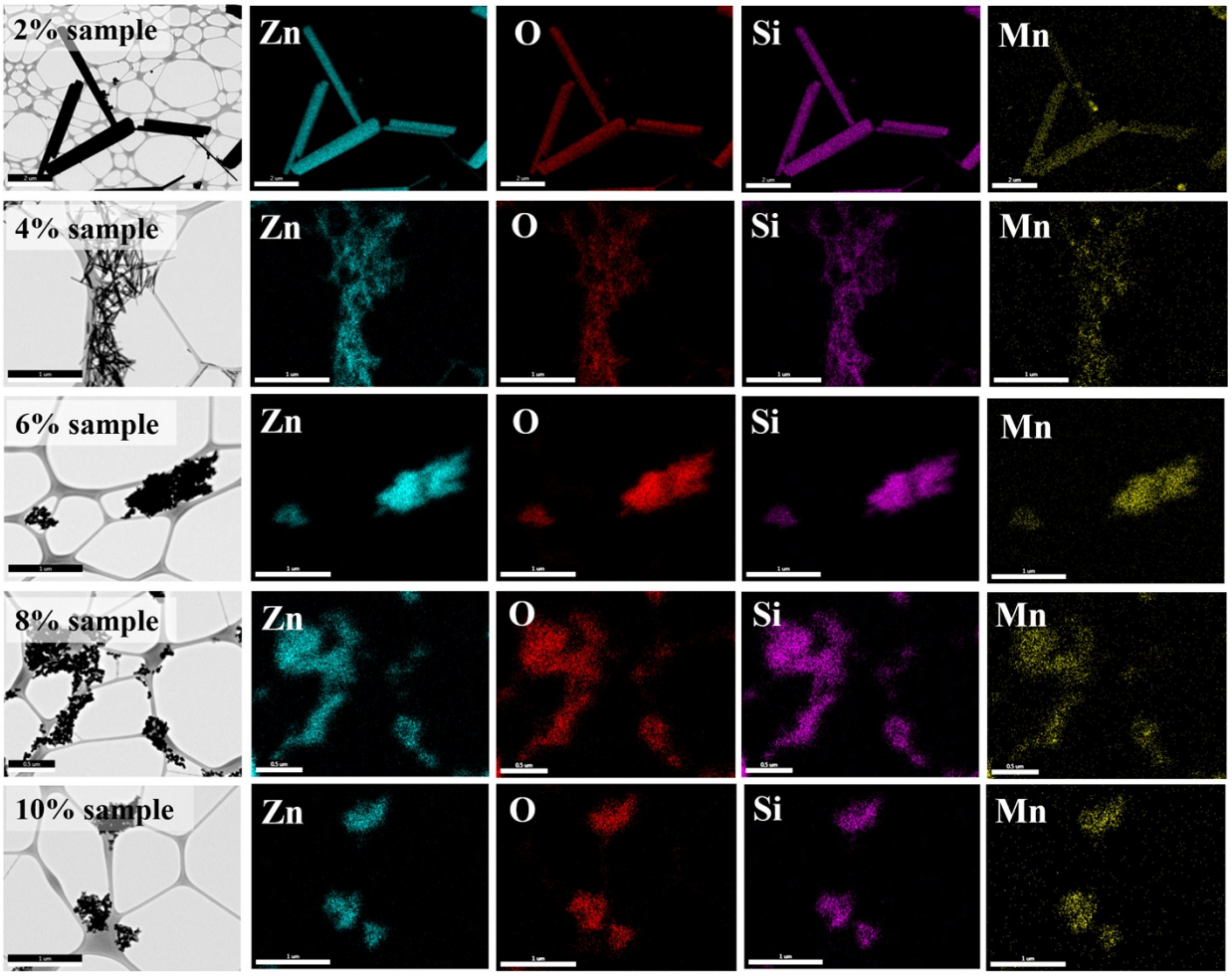


**Figure S1.** EDAX elemental mapping images of a series of as-synthesized Mn-doped $Zn_2SiO_4$ series with intended Mn dopant molar concentrations of 2%, 4%, 6%, 8%, and 10%, respectively. The scale bars in each row are 2 µm, 1 µm, 1 µm, 0.5 µm, and 1 µm, respectively.

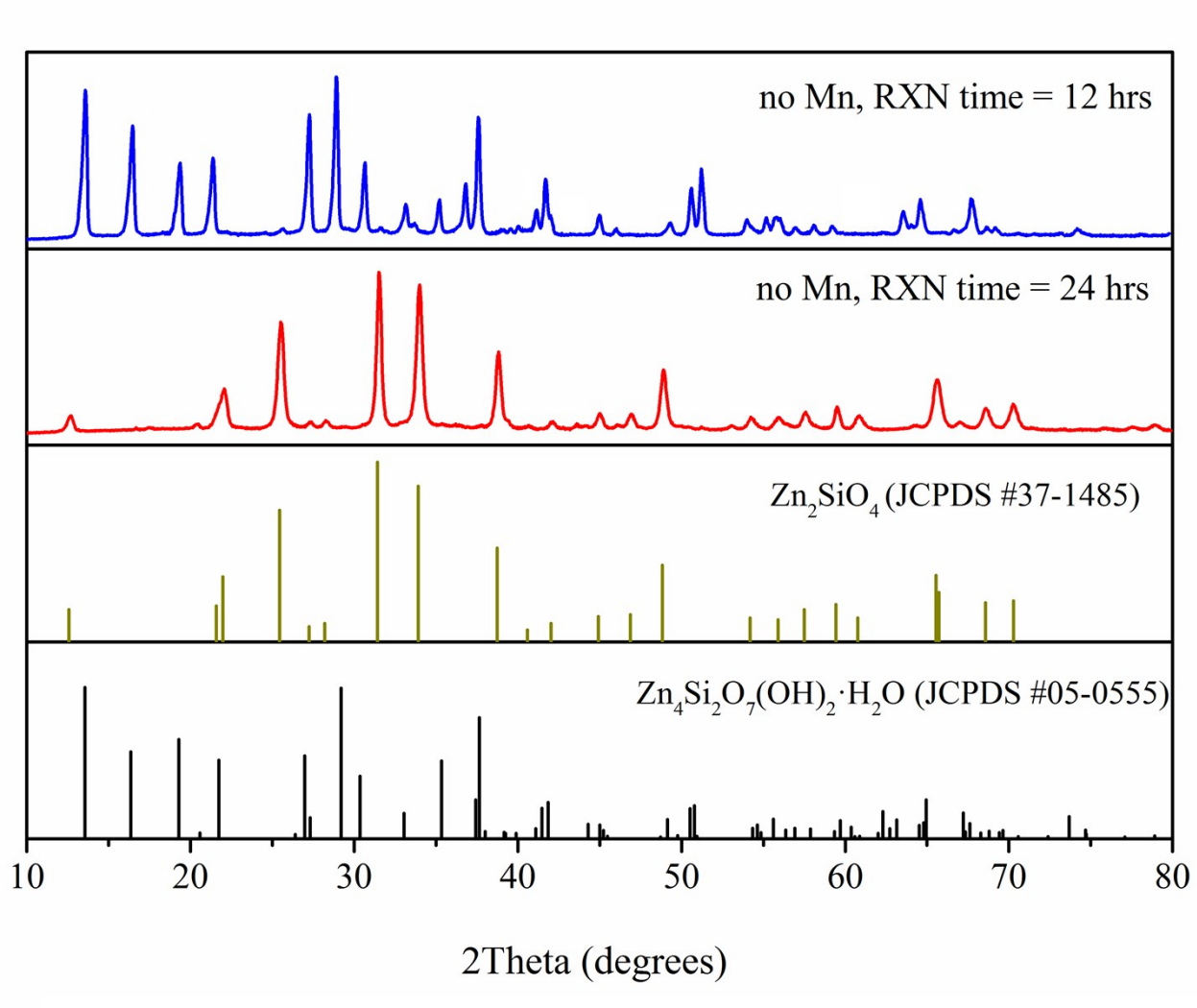


**Figure S2.** XRD patterns of a series of as-synthesized pure $Zn_2SiO_4$ samples prepared with reaction time of 12 hours and 24 hours, respectively. Database standards are shown at the bottom as JCPDS #37-1485 and 05-0555, respectively, for $Zn_2SiO_4$ and $Zn_4Si_2O_7(OH)_2 \cdot H_2O$.

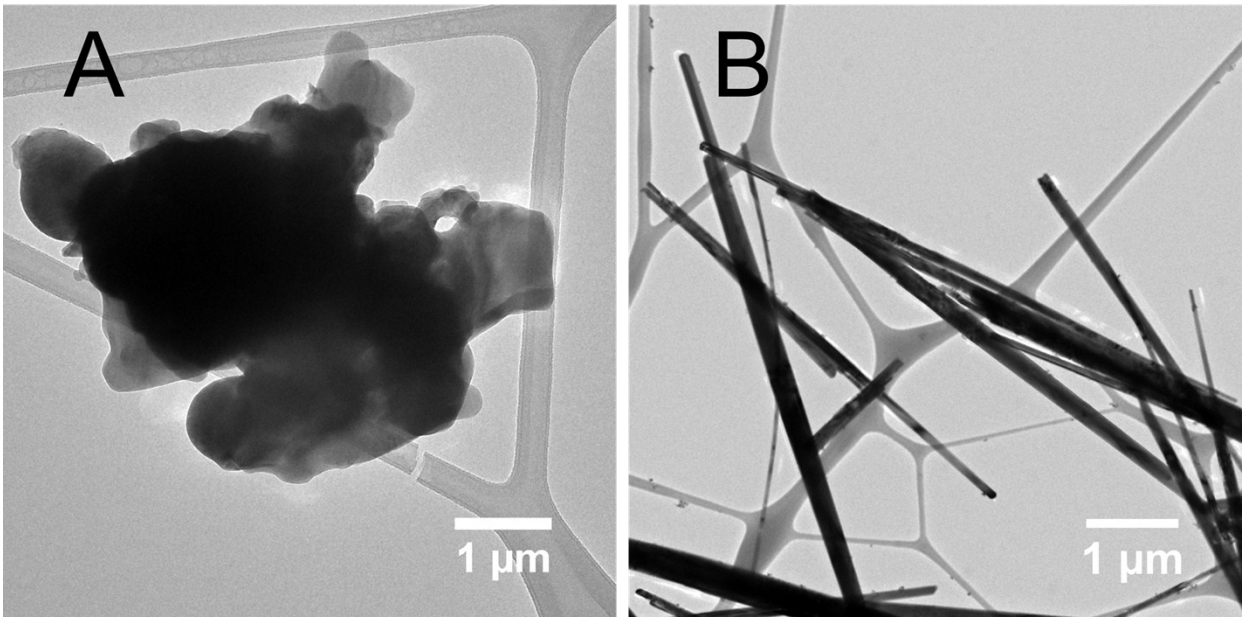


**Figure S3.** TEM images of as-synthesized pure $Zn_2SiO_4$ samples prepared with a reaction time of (A) 12 hours and (B) 24 hours, respectively.

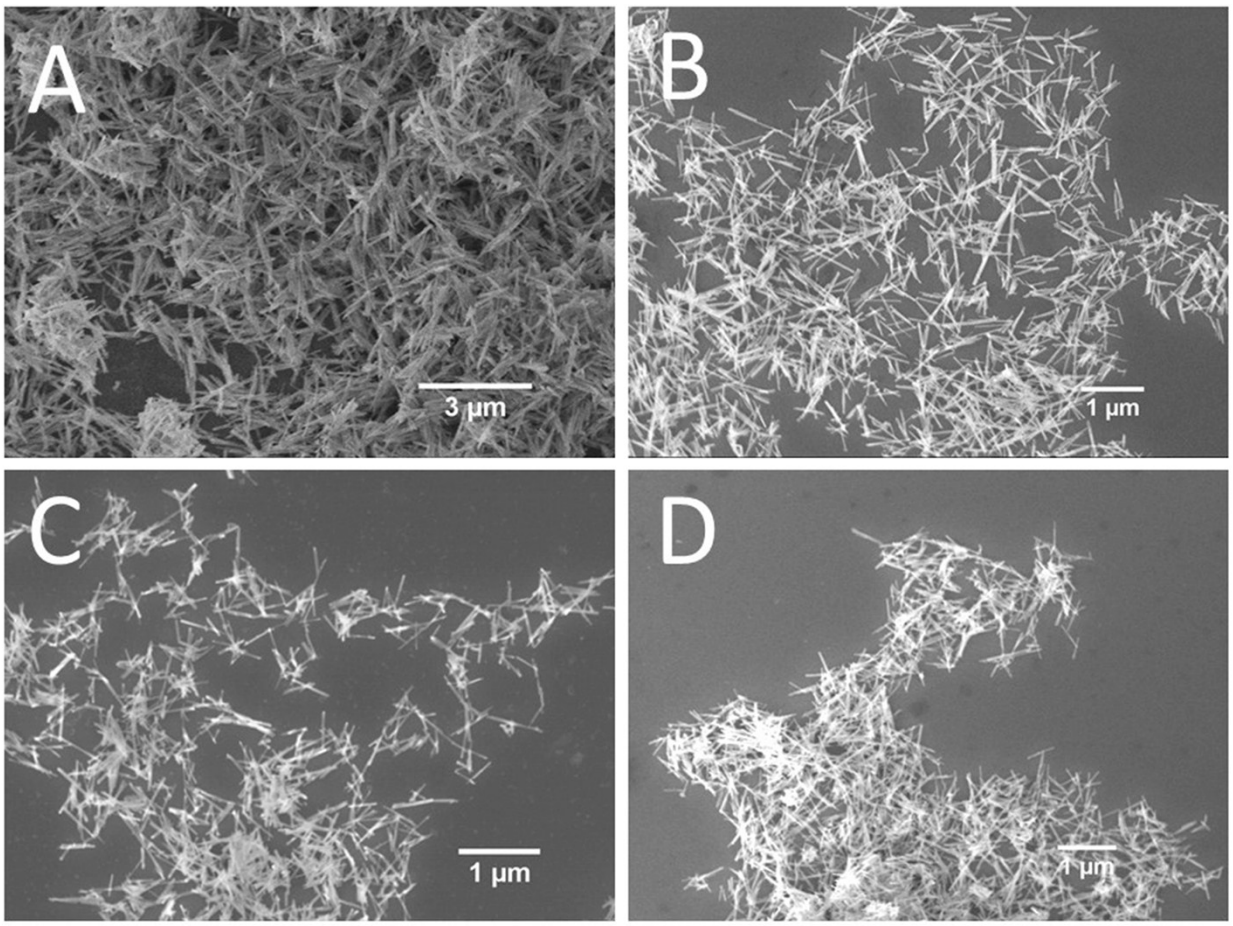


**Figure S4.** Large-scale SEM images of a series of optimized Mn-doped $Zn_2SiO_4$ samples with intended Mn dopant concentrations of (A) 3%, (B) 4%, (C) 6%, and (D) 8%, respectively.

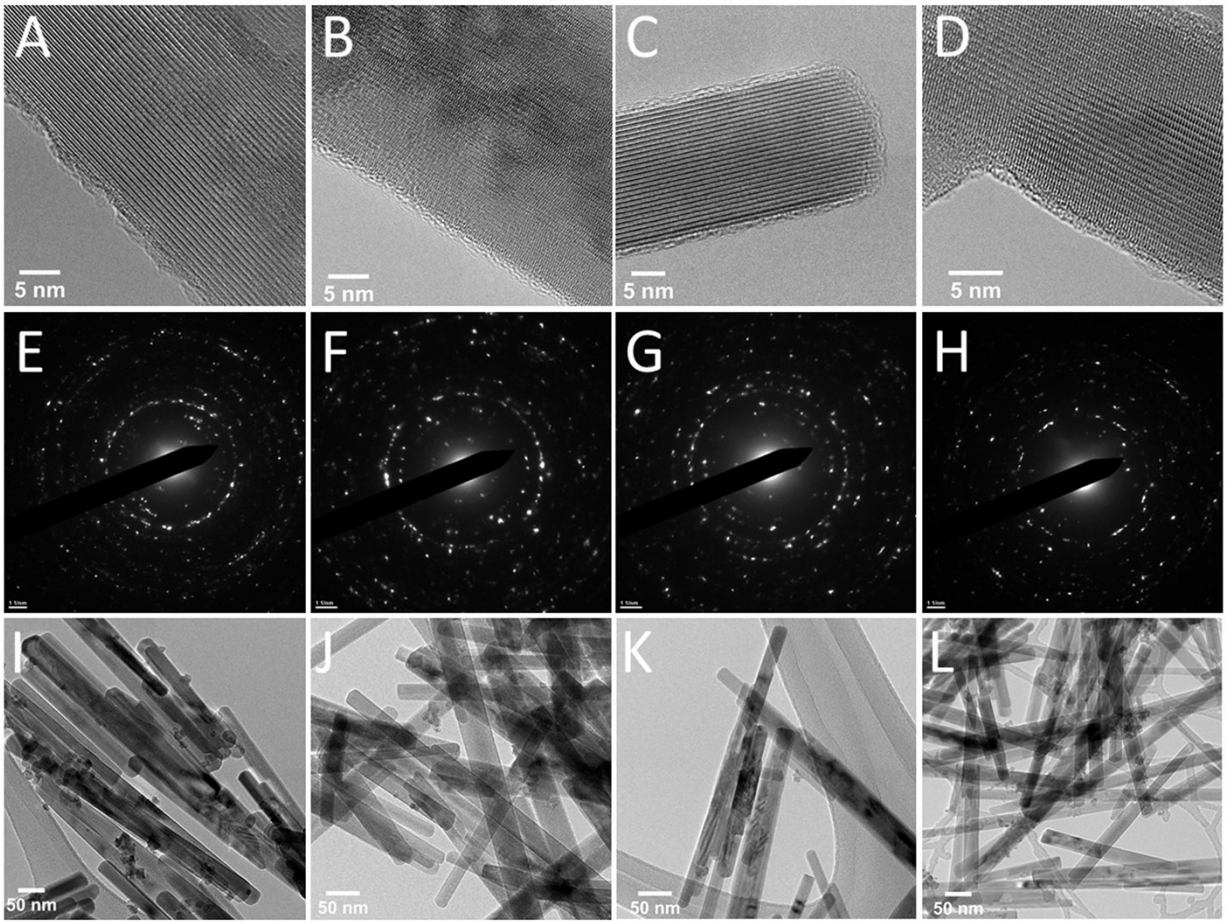


**Figure S5.** High-magnification HRTEM images (A-D) in addition to SAED patterns (E-H) and their corresponding lower-magnification HRTEM images (I-L) associated with a series of optimized Mn-doped $Zn_2SiO_4$ samples with intended Mn dopant concentrations of (A, E, I) 3%, (B, F, J) 4%, (C, G, K) 6%, and (D, H, L) 8%, respectively.

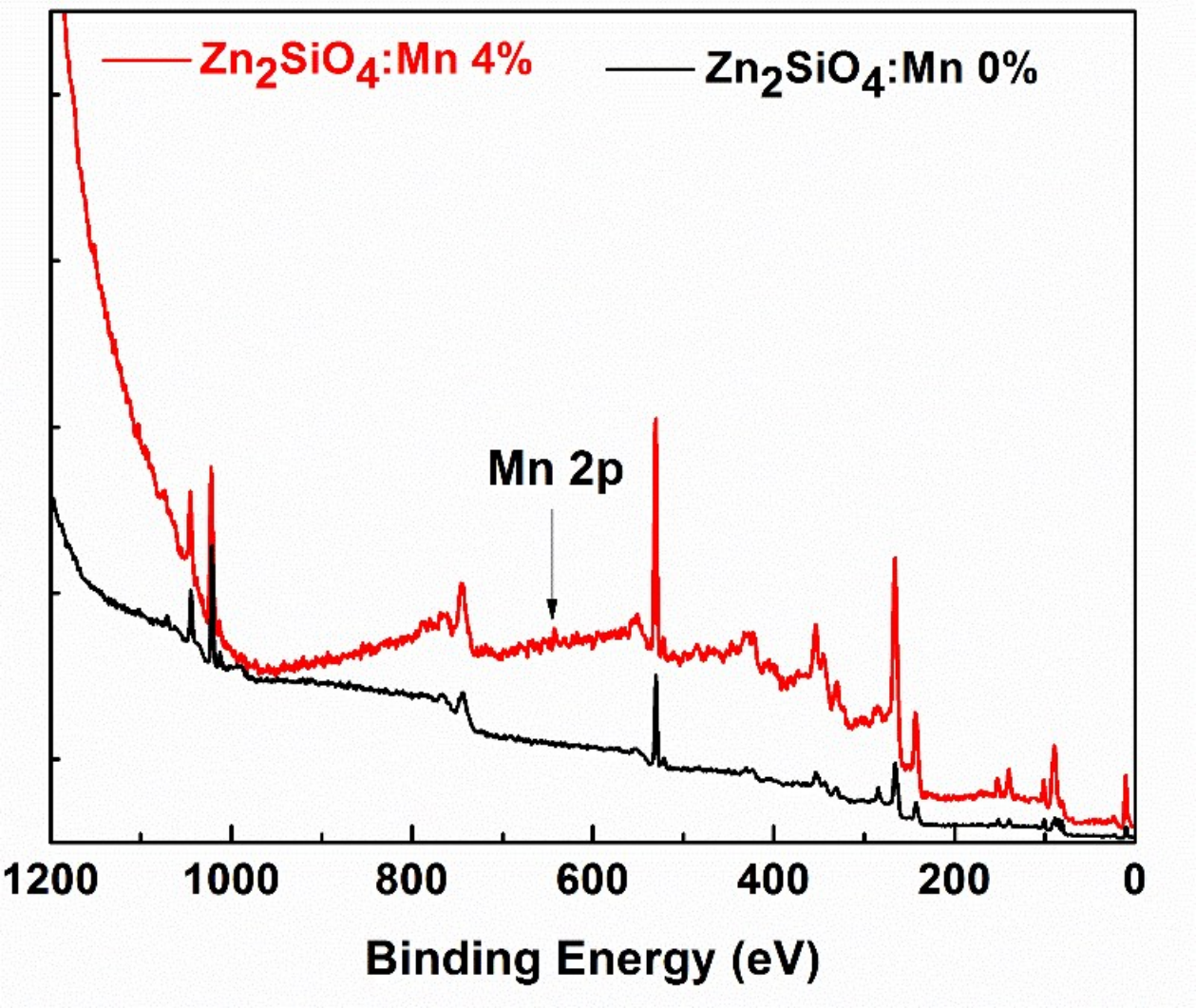


**Figure S6.** Survey spectra of as-prepared $Zn_2SiO_4$: Mn (0% undoped samples; black curve) and analogous $Zn_2SiO_4$: Mn (4% doped samples; red curve) nanorods.

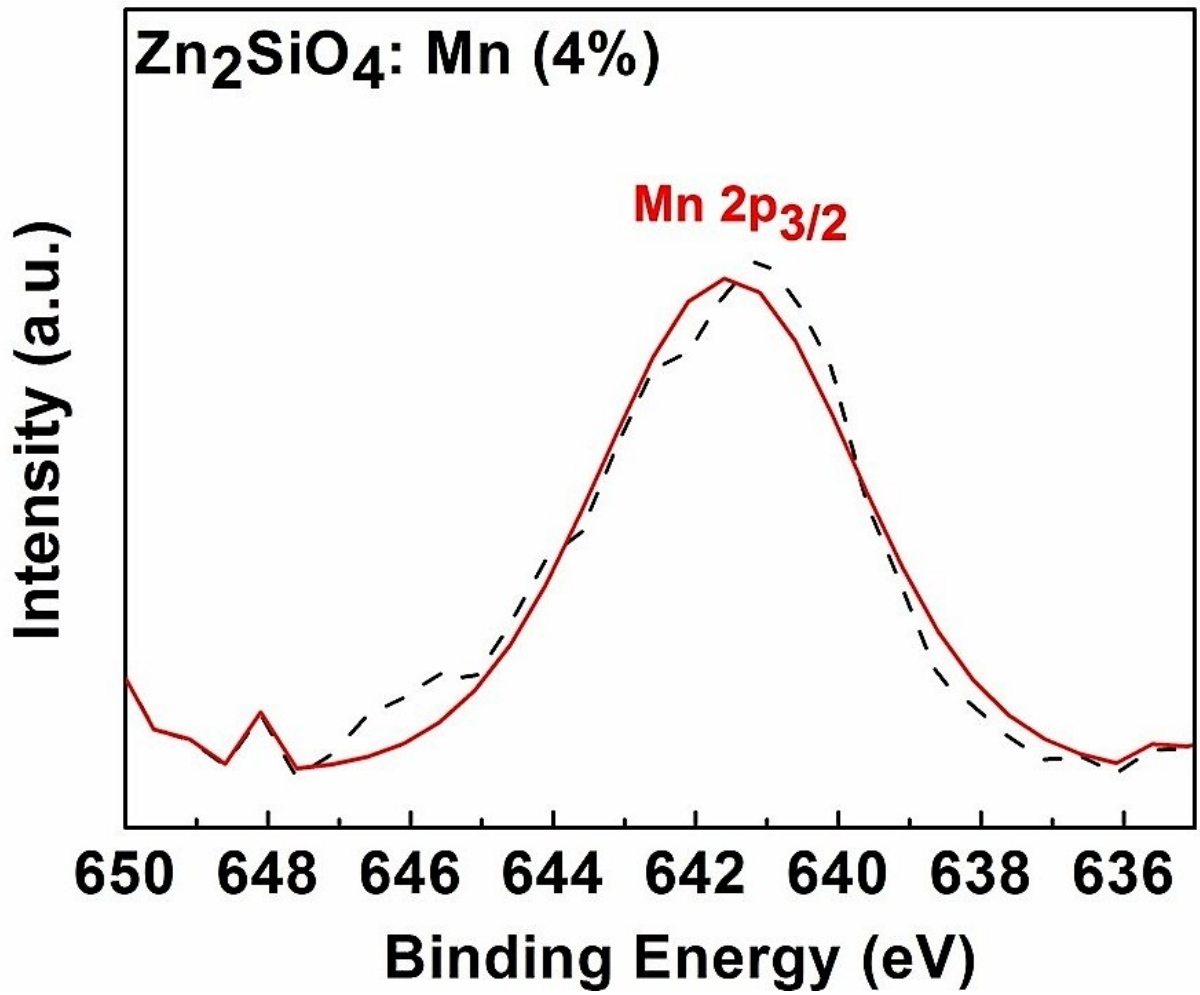


**Figure S7.** The Mn 2*p* XPS spectrum of as-prepared $Zn_2SiO_4$: Mn (4% dopant) nanorods is shown. Both the raw data (dashed black line) as well as the as-generated curve obtained after data fitting (solid red line) are highlighted.

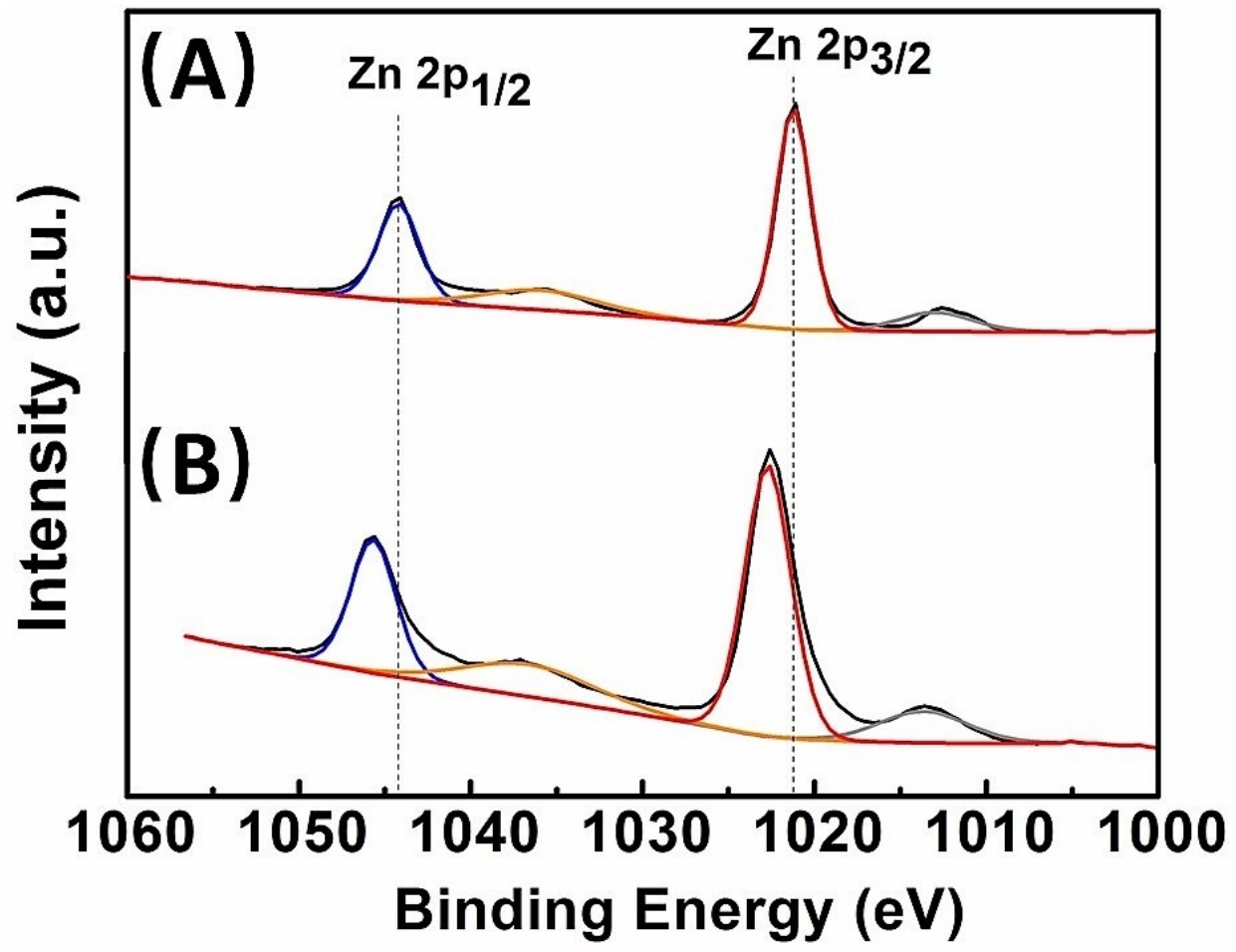


**Figure S8.** Zn 2*p* XPS spectra of (A) as-prepared $Zn_2SiO_4$: Mn (0% undoped control sample) and of corresponding (B) $Zn_2SiO_4$: Mn (4% dopant) nanorods

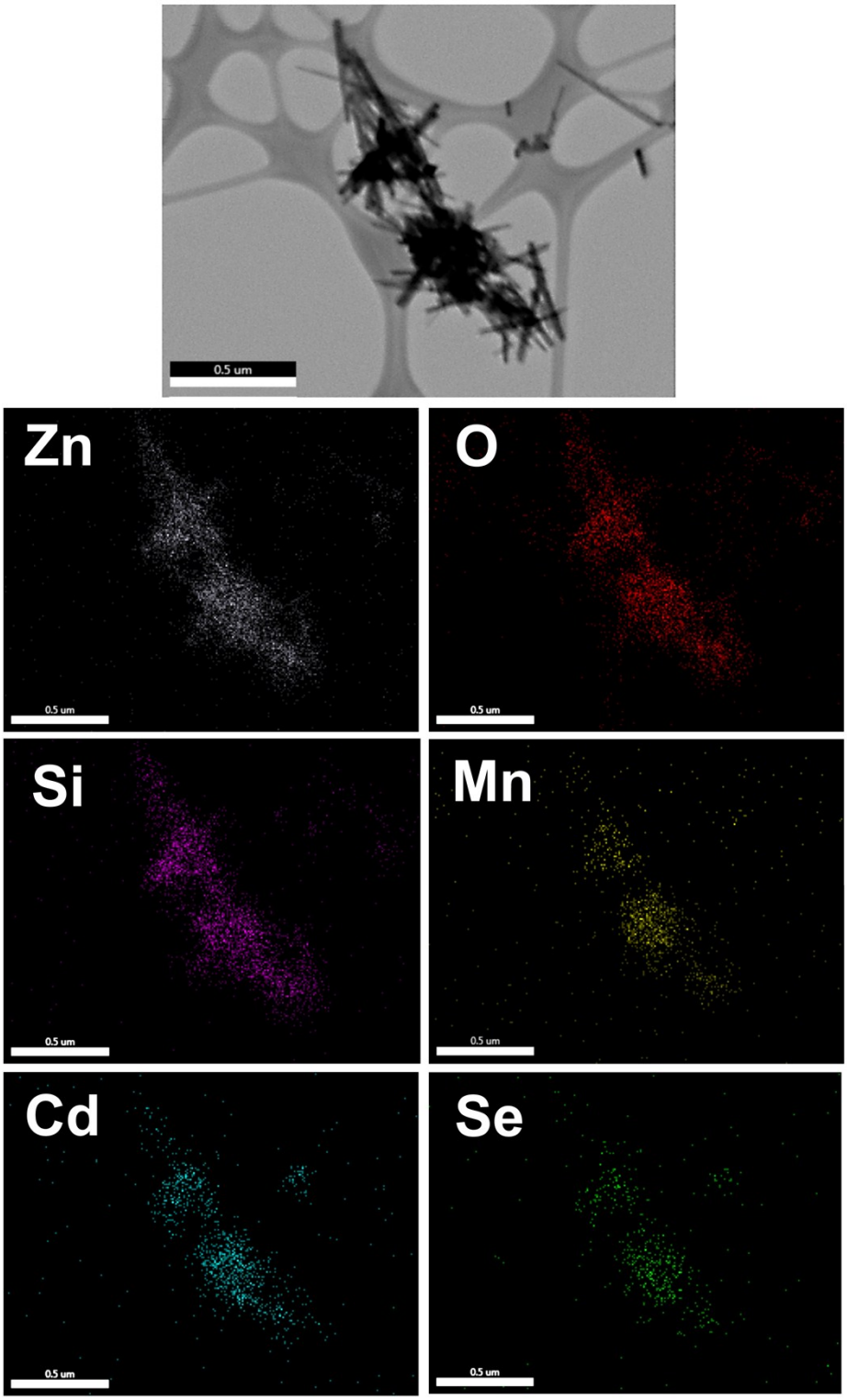


**Figure S9.** STEM image (top) as well as EDAX elemental mapping images (bottom) of the CdSe QD – Mn-doped (4%) $Zn_2SiO_4$ heterostructures.

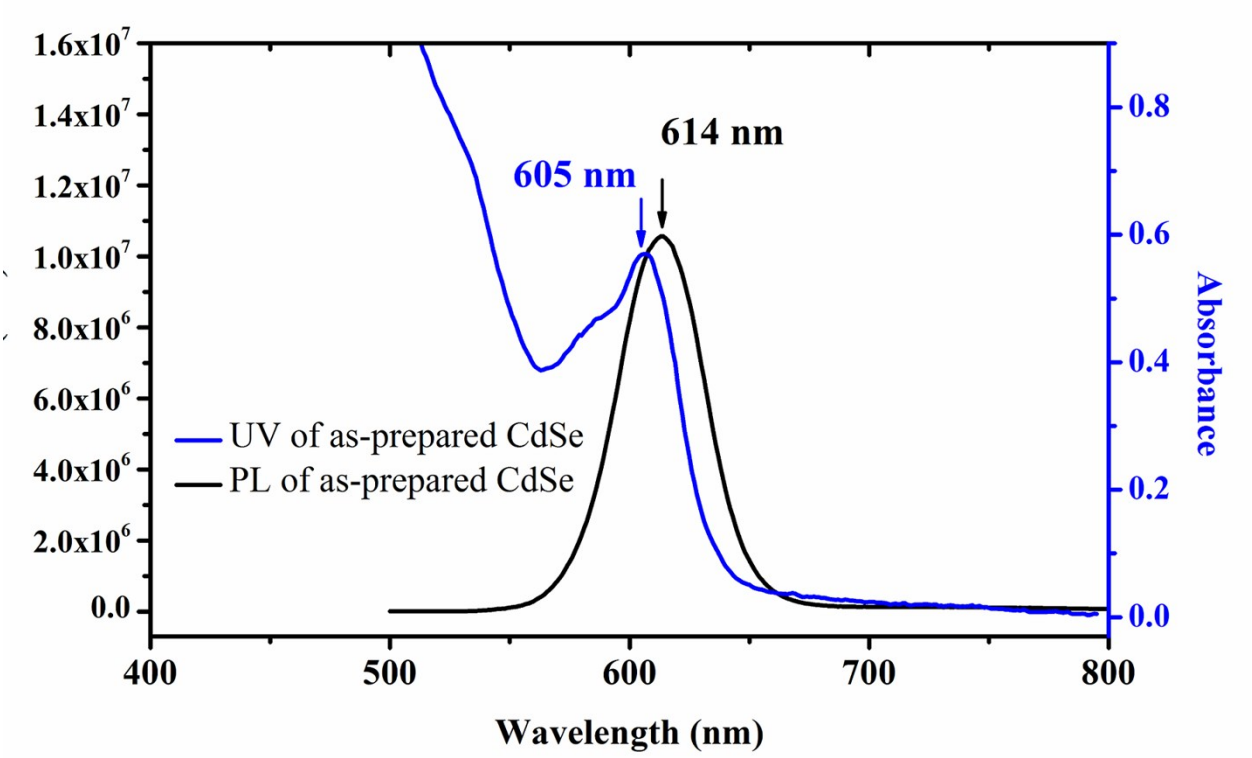


**Figure S10.** UV-visible and corresponding photoluminescent spectra of as-synthesized CdSe quantum dots. The calculated average size of the QDs is 4.8 nm.

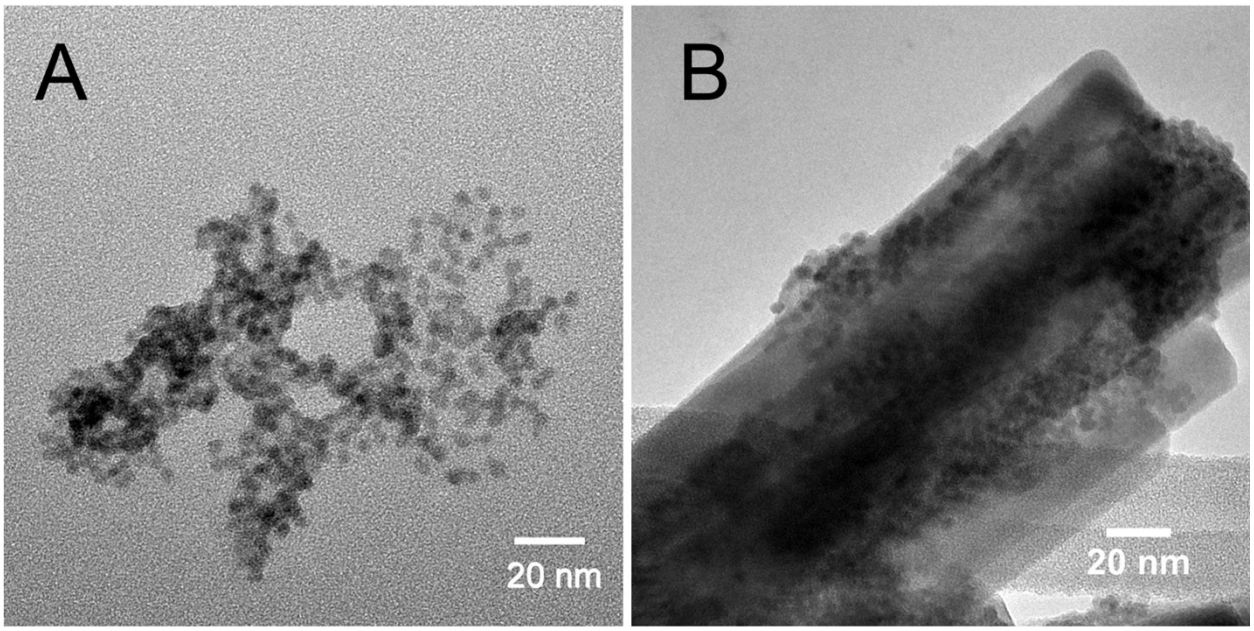


**Figure S11.** Representative TEM images of (A) MPA-capped CdSe QDs and of (B) MPA-capped CdSe QD – Mn-doped $Zn_2SiO_4$ 0D-1D heterostructures.

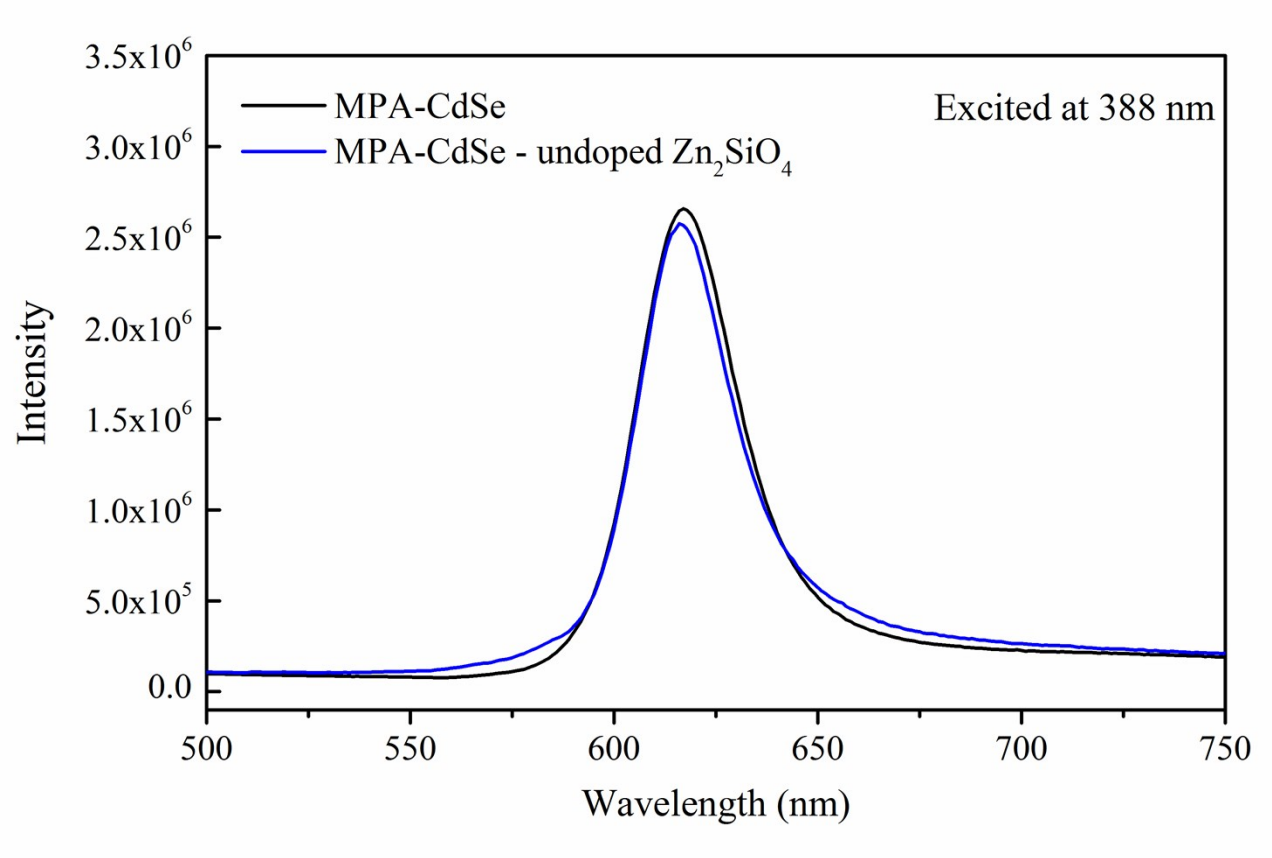


**Figure S12.** PL emission spectra of not only MPA-capped CdSe QDs (black) but also MPA-capped CdSe QD - undoped $Zn_2SiO_4$ heterostructures (blue) upon 388 nm excitation.

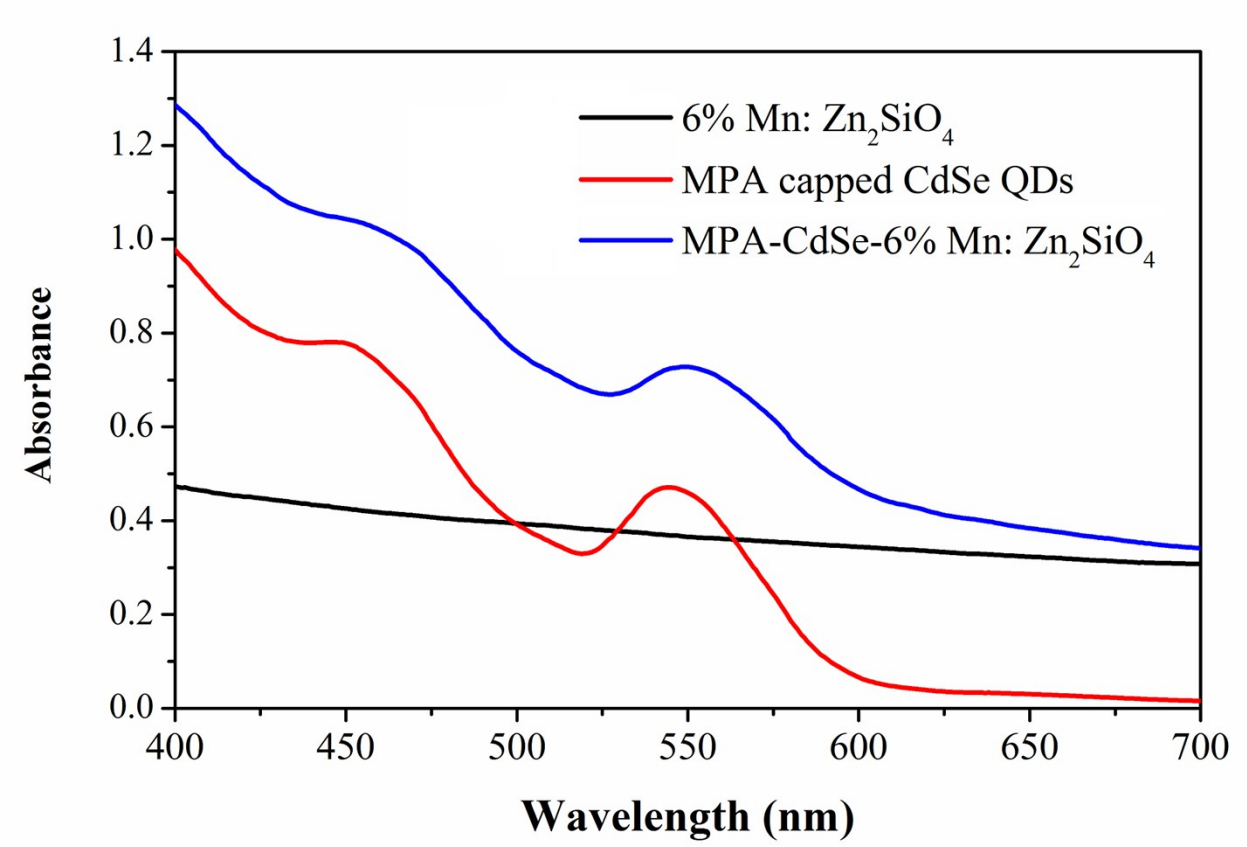


**Figure S13.** UV-visible spectra of as-synthesized 6% Mn-doped $Zn_2SiO_4$ (black), of MPA-capped CdSe quantum dots (red), and of the resulting MPA-capped CdSe QD - 6% Mn-doped $Zn_2SiO_4$ heterostructures (blue), respectively.

| **Lifetime of CdSe QDs (excited at 388 nm)** | |
|---|---|
| *Sample* | *Observed lifetimes (ns) with corresponding standard deviation values* |
| As-prepared CdSe QDs | 24.8 ( ± 0.6) |
| MPA-capped CdSe QDs | 5.7 ( ± 0.2) |
| MPA-capped CdSe QD - 4% Mn-doped $Zn_2SiO_4$ heterostructures | 3.2 ( ± 0.3) |

**Table S1.** Lifetimes of CdSe QD emission, measured at an excitation wavelength of 388 nm.